Acrylic Copolymers with Perfluoroalkylated Biphenyl Side Groups: Correlation Structure−Surface Properties

Patrice Hartmann,† André Collet, and Michel Viguier*

Laboratory Organisation Moléculaire Evolution et Matériaux Fluorés UMR-CNRS-5073, C.C 017 Université Montpellier II, Pl. E. Bataillon, F. 34095 Montpellier Cedex 05, France

Received April 21, 2006; Revised Manuscript Received July 21, 2006

ABSTRACT: We investigate the surface properties of a series of random copolymers of perfluoroalkylated biphenyl acrylates (CH_2═$CHCOO(CH_2)_mOC_6H_4C_6H_4O(CH_2)_3C_8F_{17}$, m = 0, 6, 11) and methyl methacrylate (MMA) or octadecyl methacrylate (SMA). The surface properties of the polymers were correlated to the structural parameters. Wetting hysteresis and surface tensions were estimated from dynamic contact angle measurements. It was established from atomic force microscopy analysis that wetting hysteresis cannot arise from surface anomalies. The stability of the polymer surface is enhanced by the presence of biphenyl groups and octadecyl side chains in SMA copolymer series. Surface tensions of polymers were calculated using different methods involving the Lifshitz−van der Waals/acid−base approach (van Oss et al.) and the equation of state (Neumann et al.). The low surface tensions (ca. 11 mN/m) depend on three main structural parameters: copolymer composition, type of comonomer, and length of hydrocarbon spacer $(CH_2)_m$.

1. Introduction

Comblike acrylic polymers with pendent perfluoroalkyl groups have found numerous applications as oil- and water-repellent coatings.[1,2] Surface tensions (γ) of these polymers ($\gamma \approx 10-15$ mN/m) are lower than that of PTFE, despite the latter containing a higher fluorine ratio. These remarkable surface properties are explained by the presence of CF_3 end groups in the outermost part of the surface and by a higher density of fluorine at the polymer interface than in the bulk. Studies carried out by angle-dependent X-ray photoelectron spectroscopy have clearly shown that the concentration profile of fluorine exhibits a steep gradient decreasing from the polymer−air interface.[3−5] The higher fluorine concentration in the outermost surface (3.8 nm) of fluorinated acrylic copolymers has been recently confirmed by low-energy ion scattering (LEIS).[6] The migration of perfluoroalkylated groups arises from the phase segregation occurring between perfluorinated segments and polymer matrix. This process tends to reduce the surface free energy and is favored by a thermodynamic factor.

The wettability of the polymer surface by various wetting liquids can be quantified by contact angles measurements. The surface tensions are often estimated from dynamic advancing contact angles (θ_a). One would expect unique and constant values of contact angles. However, the surface wettability of polymers evolves when in contact with liquids and particularly with polar liquids such as water. The discrepancy ($\Delta\theta$) between the advancing (θ_a) and receding (θ_r) contact angles, referred to as wetting hysteresis, reveals an increase in the wettability due to the reorganization of the polymer surface, when in contact with the wetting liquid. The surface properties of perfluoroalkylated acrylic comblike polymers are directly linked to the organization of the perfluoroalkyl groups in the outermost part of the surface.[3−7] In the low wetting state, the perfluorinated groups are regularly packed, parallel to each other forming lamellae. In the high wetting state, the perfluorinated groups are irregularly arranged at the surface, and lower contact angles are observed. The reorientation of the perfluorinated side groups can largely be explained by the weak cohesive energy between perfluorinated chains.[8]

The self-organization of comb-shaped polymers depends on structural parameters: nature of the polymer backbone, size of the pendent perfluorinated tail, and length of the hydrocarbon spacer.[9−17] As related for comb-shaped liquid crystal polymers,[18] the anisotropic organization of the rodlike pendent end groups depends, in a critical way, on the combination of backbone and spacer relative flexibilities. Previous studies devoted to the specific role of the hydrocarbon spacer in the wettability of perfluoroalkylated acrylic polymers have shown that the wetting hysteresis was minimum ($\Delta\theta \leq 20°$) for short [$(CH_2)_2$] or long [$(CH_2)_{10}$ or $(CH_2)_{11}$] hydrocarbon side groups. The lower wetting hysteresis was correlated with the highest side-chain organization established by X-ray diffraction.[19]

Incorporation of nonfluorinated alkyl acrylate monomer units into perfluoroalkylated acrylic chain can modify the wetting behavior. This is of outmost importance in terms of practical applications. The surface free energy of random copolymers (i.e., poly(perfluoroalkylethyl acrylate-*co*-*n*-alkyl acrylate)s) estimated from dynamic advancing contact angles does not significantly depend on the alkyl side chain length. However, the wetting hysteresis decreases as the length of the alkyl chain reaches 10 carbons or more in relation with the development of crystallinity.[20]

The correlation between organization of perfluoroalkylated (or any long alkyl side chains) and surface stability suggests that tailoring of the surface properties may be controlled by a pertinent selection of side chains. In this paper we investigate the wetting behavior and surface tension of a series of acrylic copolymers of perfluoroalkyl acrylates ($F8BPH_mA$) and MMA or SMA (cf. Scheme 1) by contact angle measurements. To limit the molecular reorganization of the polymer surface, a biphenyl mesogenic group was introduced between the perfluorinated end groups and the hydrocarbon spacer. As shown recently, the self-ordering tendency of the mesogenic biphenyl core is enhanced

† Present address: UNESCO Associated Centre for Macromolecules, Department of Chemistry and Polymer Science, University of Stellenbosch, Private Bag X1, 7602 Stellenbosch, South Africa.

* To whom correspondence should be addressed: e-mail mviguier@univ-montp2.fr; Tel 33-467 14 32 13; Fax 33-467 63 10 46.

10.1021/ma060894t CCC: $33.50
Published on Web 09/12/2006

Scheme 1. Structures of Copolymers

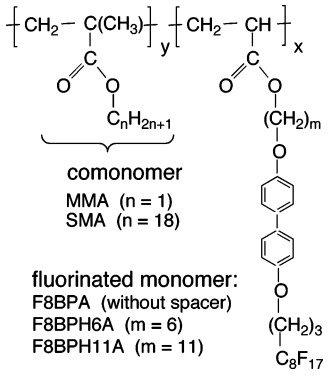

by perfluorinated groups.[21] A synergistic effect on the cohesive energy between side chains was expected from the association of the rodlike perfluorinated end group and the mesogenic biphenyl core.

2. Materials and Methods

2.1. Materials. Biphenyl-containing monomers were prepared using biphenol (Avocado, 99%) as starting compound. The synthesis of the perfluoroalkylated monomers (cf. Scheme 1) 4-(acryloyloxy)-4′-(3-perfluorooctylprop-1-yloxy)biphenyl (F8BPA), 4-(6-acryloyloxyhex-1-yloxy)-4′-(3-perfluorooctylprop-1-yloxy)biphenyl (F8BPH6A), and 4-(11-acryloyloxyundec-1-yloxy)-4′-(3-perfluorooctylprop-1-yloxy)biphenyl (F8BPH11A) have been described previously.[21] 2,2′-Azobis(isobutyronitrile) (AIBN) was recrystallized from methanol before use.

2.2. Polymerization Procedure. Copolymers were synthesized by free radical polymerization in butyl acetate at 80 °C for 6 h, using 2 mol % of AIBN as initiator. The reaction mixture was degassed under vacuum using three freeze/thaw cycles. The polymers were precipitated twice into methanol and dried under reduced pressure. The polymers were obtained as white powders (yield ≈ 70%).

2.3. Bulk Characterization Techniques. Molecular weights were determined by size exclusion chromatography (SEC) using a Varian 2510 HPLC apparatus equipped with a refractive index detector Shimadzu RID-6A. The column set was constituted of three PL Gel columns (Polymer Laboratories) with pore sizes 10^4, 10^3, and 500 Å. THF was used as the eluent with a flow rate of 1 mL/min (P = 45 atm).

The relative calibration plot was calculated with polystyrene standards. Most of the copolymers synthesized up to 50 or 55 mol % of fluorinated units were fully soluble in THF, allowing the analysis by SEC with THF as eluent. A monomodal distribution of molecular weights is observed with a polydispersity index ranging between 1.7 and 3.3.

^{1}H NMR spectra were recorded on a Brücker 250 MHz spectrometer. The experimental ratio of fluorinated monomer units was calculated from the ^{1}H NMR spectra and based on the resonance of aromatic protons (δ = 6.9−7.6 ppm) and alkoxy protons (CH_3O or CH_2O) (δ = 3.6−4.2 ppm). ^{1}H NMR and SEC analysis confirmed the absence of monomer in the purified polymer.

The X-ray diffraction experiments were performed using a Philips diffractometer equipped with a nickel monochromator and a copper anticathode (Kα 1.5418 Å). Samples were prepared from freshly precipitated and dried polymers, reduced in powder, and compacted on a glass plate.

The thermal behavior of copolymers was studied by differential scanning calorimetry (DSC) using a Mettler DSC-30 calorimeter with heating rates of 10 °C/min.

2.4. Surface Characterization Techniques. AFM observations were carried out using an Autoprobe CP Research apparatus from T M Microscopes-Veeco.

Contact angle measurements were performed at 20 °C using the Wilhelmy plate method with a Lauda tensiometer. Polymer surface samples were prepared by dip-coating on optical microscopy cover slides (18 × 18 mm) from solutions of polymer in chloroform. Glass cover slides were previously cleaned by a brief immersion in aqueous HF 10%, then washed several times in purified water, and dried at 150 °C under vacuum. Polymer coatings were dried at 120 °C under vacuum and slowly cooled to room temperature. The dynamic contact angles were determined from the immersion and emersion plateaus of the wetting diagram obtained with a wetting/dewetting velocity of 0.5 mm/min. At least three wetting diagrams by copolymer sample were carried out to confirm the reproducibility of the advancing (θ_a) and receding (θ_r) contact angles measurements. The surface tensions of wetting liquids used as standards were controlled using the Du Noüy ring method: $\gamma_L(C_8H_{18}) = 21.6$ mN/m, $\gamma_L(CH_2I_2) = 50.8$ mN/m, $\gamma_L(H_2O) = 72.8$ mN/m, and $\gamma_L(EG) = 48.0$ mN/m. Values from the literature[22] were used for the Lifshitz−van der Waals component γ_i^{LW} and Lewis acid (γ_i^+) and base (γ_i^-) components: water ($\gamma_L^{LW} = 21.8$ mN/m and $\gamma_L^+ = \gamma_L^- = 25.5$ mN/m) and ethylene glycol ($\gamma_L^{LW} = 29.0$ mN/m, $\gamma_L^+ = 1.9$ mN/m, and $\gamma_L^- = 47.0$ mN/m).

To remove surface contaminants, the ring was immersed in chromic acid, carefully rinsed with deionized water, and finally flamed before use. Water for contact angle measurements was distilled and passed through a Milli-Q (Millipore) ion exchange column. Diiodomethane (Alfa Aesar) was purified by passing over a column of silica (Merck) with particle sizes 40−60 μm. Octane and ethylene glycol (Aldrich) were used as received.

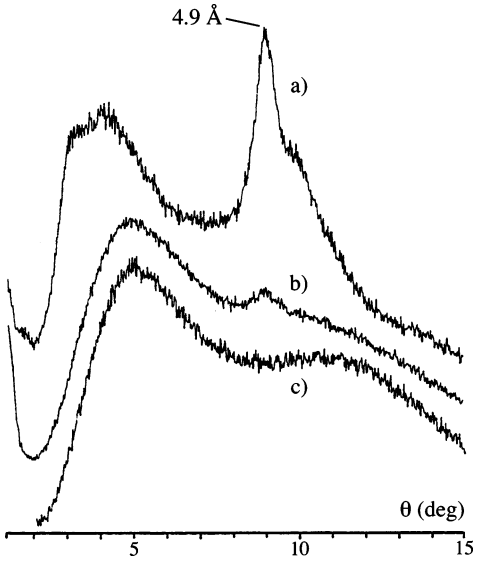

Figure 1. X-ray scattering patterns of copolymers p(F8BPH$_m$A-*co*-MMA): (a) p-F8BPH11A-*co*-MMA 50%, (b) p-F8BPH6A-*co*-MMA 50%, (c) p-F8BPA-*co*-MMA 54%.

3. Results and Discussion

As outlined previously, the relationship between the side-chain organization and the wetting behavior is well established. However, the correlation between surface properties (surface tension, wetting hysteresis) and structural parameters is less well understood. The structural parameters studied through the different series of copolymers are in relation to the nature of hydrocarbon side chain of comonomers, methyl (MMA) or octadecyl (SMA), the fluorinated monomer content, and the length of the hydrocarbon spacer [$(CH_2)_m$ with m = 0, 6, 11] linking the biphenyl core and the acrylic group.

3.1. Bulk Organization from X-ray Studies. In a recent paper,[21] we established, from differential scanning calorimetry (DSC) that homopolymers p(F8BPHmA)with hydrocarbon spacers $(CH_2)_6$ or $(CH_2)_{11}$ exhibit a more pronounced ability to organize in bulk. This tendency was confirmed by X-ray diffraction (WAXD) measurements. Figure 1 shows WAXD

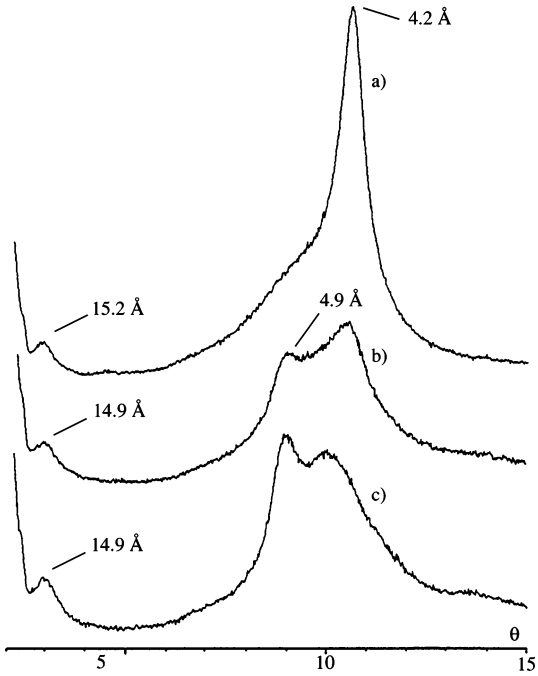

Figure 2. X-ray patterns of copolymers p(F8BPH$_{11}$A-*co*-SMA): (a) p-F8BPH11A-*co*-SMA 10%, (b) p-F8BPH11A-*co*-SMA 31%, (c) p-F8BPH11A-*co*-SMA 46%.

patterns for p(F8BPHmA-*co*-MMA) copolymers with different hydrocarbon spacers. Because of the presence of MMA comonomer, the organization of fluorinated side chain was drastically reduced. Nevertheless, for a higher fluorinated content (50 mol %) the X-ray pattern of the copolymer p(F8BPH$_{11}$A-*co*-MMA) presents a narrow peak with a *d* spacing of 4.9 Å, which is characteristic of the distance between regularly packed perfluoroalkyl chains. This result is consistent with the transition observed by DSC at $T = 140.1$ °C. In the p(F8BPH$_6$A-*co*-MMA) series, DSC thermograms of copolymers with 50 and 75 mol % of fluorinated units, present transitions at $T = 114.2$ °C ($\Delta H = 1.1$ kJ/mol) and $T = 130.3$ °C ($\Delta H = 2.4$ kJ/mol), respectively, attributed to the organization of fluorinated side groups. Copolymers containing fluoromonomer F8BPA, without hydrocarbon spacer, present X-ray patterns with broad and diffuse reflections and no transition on DSC thermograms, indicating a significantly low degree of order of fluorinated side chains.

As shown in Figure 2, the shape of the diffraction peak changes with the composition of copolymers with stearyl methacrylate. The X-ray diffraction plot of low fluorinated copolymer p(F8BPH$_{11}$A-*co*-SMA)-10/90 presents a narrow reflection with a *d* spacing of 4.2 Å. Such a signal is generally observed when hydrocarbon side chains are regularly packed. As the F8BPH$_{11}$A content increases, the X-ray diffraction signals become weaker and broader. At the same time, a new peak emerges ($d = 4.9$ Å) and increases with the fluorine content in copolymer, indicating the onset of the organization of the perfluorooctyl groups. As shown by DSC experiments, the enthalpies of the transition, due to the organization of stearyl side groups, decrease with the fluoromonomer content (cf. Figure 3).

The presence of fluorinated side groups perturbs the organization of stearyl side chains. The additional X-ray diffraction peaks at $d \approx 15$ Å, observed also for copolymers p(F8BPH$_6$A-*co*-SMA) but not in p(F8BPA-*co*-SMA) series, could be attributed to the layering order structure of perfluorinated groups. The organization of fluorinated side groups was also underscored, in copolymers series p(F8BPH$_6$A-*co*-SMA), by a transition at $T = 146.7$ °C. These results are consistent with DSC experiments previously published,[21] showing that the flexibility of hydrocarbon spacers could favor the decoupling between polymer chain and mesogenic side groups and in this way enhance the structural ordering of pendent chains in the polymer matrix. Conventional or fluorinated comblike homopolymers with mesogenic moieties in side groups are well-known for their ability to form nematic or smectic lamellar structures.[10,13,14,17] For polyacrylates containing spaced fluoroalkylphenyl side chains, an end-to-end arrangement in a double-layer smectic structure was suggested.[16] When observed by polarizing optical microscopy, the copolymers studied did not display clearly typical texture of a mesomorphic phase. As shown by X-ray diffraction and DSC measurements, the organization of fluorinated biphenyl side chains in copolymer series (F8BPH$_m$A)$_x$(SMA)$_{1-x}$ was favored by larger values of *x* while the packing of octadecyl side chains was enhanced by lower values of *x*.[23]

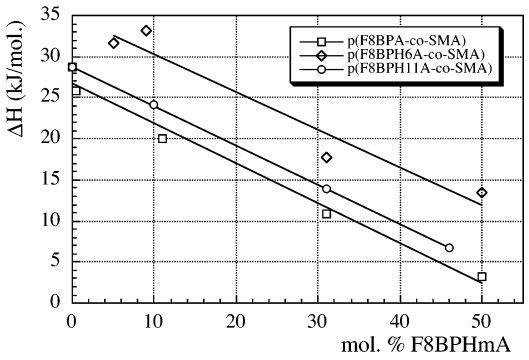

Figure 3. Thermal behavior of copolymers p(F8BPH$_{11}$A-*co*-SMA). Enthalpy of the transitions were determined from the DSC thermograms as a function of fluoromonomer content in the copolymer. ΔH is expressed in kJ/mol of SMA monomer unit.

3.2. Surface Properties. 3.2.1. Surface Topography Observed by AFM. Surface topography of the copolymer films, which should be one of the crucial parameters responsible for wetting hysteresis, was examined by AFM using the tapping-mode method. Figure 4 shows 3D topographic AFM images of film surfaces for copolymers p(F8BPH$_6$A-*co*-SMA) (9/91) and p(F8BPH$_{11}$A-*co*-MMA) (31/69) with scanning areas of 50 μm $\times$ 50 μm. The surfaces present few topographic defects whose amplitude does not exceed 30 nm. The root-mean-square (rms) roughness was 4.57 and 1.95 nm, respectively. This indicates that the influence of the surface roughness on the contact angle measurements and wetting hysteresis can be considered as negligible.[24−26]

3.2.2. Surface Wettability in the Presence of Water and Wetting Hysteresis. To investigate the wettability and the stability of copolymer surfaces, dynamic contact angle measurements were performed at low rate (0.5 mm/min). Under these conditions advancing contact angles can be considered independent of the velocity of the immersion process.[27,28] The onset of a rate dependent regime occurs at higher velocities (5 mm/min).[29] Only advancing contact angles obtained on a dry surface (θ_a determined from the first wetting cycle) is appropriate for the calculation of the surface tension. As can be seen from Table 1, a very low fluoromonomer content (mole ratio < 1%) was found to be enough to raise the advancing contact angle of p-SMA homopolymer. For a further increase of fluoromonomer content in copolymers (about 10 mol %) a plateau was rapidly reached ($\theta_a \approx 120°$). Whatever the copolymer composition (fluoromonomer contents, up to 50 mol %) and the length of

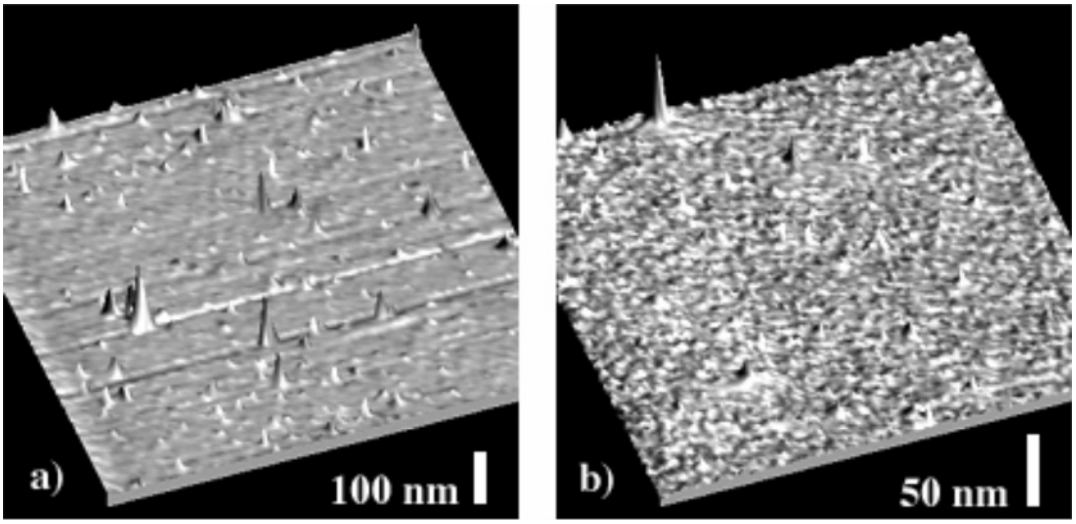

Figure 4. 3D atomic force microscopy images with a scanning size of 50 μm × 50 μm: (a) copolymer F8BPH$_6$-*co*-SMA with 9 mol % of fluoromonomer content; (b) copolymer F8BPH$_{11}$-*co*-MMA with 31 mol % of fluoromonomer content.

Table 1. Low-Rate Contact Angle Data and Wetting Hysteresis of Water for Copolymers pF8BPH$_m$A-*co*-SMA and pF8BPH$_m$A-*co*-MMA

		contact angle (deg)		wetting hysteresis	
(co)polymer	% F8BPH$_m$A	θ_a	θ_r	$\Delta\theta$	H
pSMA	0	108.9	100.0	8.9	0.082
pF8BPA-*co*-SMA	0.5	112.4	96.6	15.8	0.140
	11	121.5	106.5	15.0	0.123
	31	126.5	96.4	30.1	0.238
	50	125.7	104.5	21.2	0.169
pF8BPH$_6$A-*co*-SMA	0.5	113.3	94.9	18.4	0.162
	5	113.9	94.9	19.0	0.167
	9	123.0	104.2	18.8	0.153
	31	125.1	106.5	18.6	0.149
	50	125.4	109.2	16.2	0.129
pF8BPH$_{11}$A-*co*-SMA	10	120.1	102.1	18.0	0.150
	31	125.9	96.1	29.8	0.237
	46	128.2	107.4	20.8	0.162
pMMA	0	78.9	56.1	22.8	0.289
pF8BPA-*co*-MMA	10	118.0	90.6	27.4	0.232
	34	123.4	100.3	23.1	0.187
	54	125.7	99.0	26.7	0.212
pF8BPH$_6$A-*co*-MMA	9	124.4	89.1	35.3	0.284
	31	127.3	104.1	23.2	0.182
	50	124.6	106.9	17.7	0.142
pF8BPH$_{11}$A-*co*-MMA	12	124.9	100.8	24.1	0.193
	31	126.0	94.4	31.6	0.250

the hydrocarbon spacer (H$_m$), the values of θ_a reached a maximum ranging between 125° and 130°.

Contact angle hysteresis can be expressed by different relations: the arithmetic difference $\Delta\theta = \theta_a - \theta_r$ or a dimensionless form,[30] referred to as reduced hysteresis H, $H = (\theta_a - \theta_r)/\theta_a$. Values of the reduced hysteresis H were independent of the wetting liquid.[31] Wetting hysteresis was more sensitive to the chemical structure of the fluorinated side chains than the advancing contact angles (cf. Table 1). Most of the copolymers presented low wetting hysteresis values ($\Delta\theta \leq 20°$, $H \leq 0.250$) in comparison with perfluoroalkyl ethyl/*n*-alkyl acrylic copolymers.[20]

The most frequent causes cited to explain contact angle hysteresis are surface roughness, chemical inhomogeneity, diffusion of liquid into the polymer, and polymer swelling and molecular reorientation of polymer side chains at the interface.[32]

In this study wetting hysteresis cannot be ascribed to surface roughness. Polymer surface topography examined by AFM presented submicrometer size defects which are far less than the dimension required to significantly contribute to contact angle hysteresis.

Estimated from WAXS analysis, the size of domains of organization of pendent chains (perfluoroalkylated or octadecyl) did not exceed 100 Å. The formation of microdomains with specific chemical composition will improve the side group organization. A priori the influence of the chemical heterogeneity or roughness cannot be completely excluded, but it seems unlikely that it could be the main cause of the observed wetting hysteresis. Furthermore, the Wilhelmy method used to determine contact angles involves a large moving three phase contact line that may alleviate the effect of local chemical or topographic irregularities on the polymer surface.

The penetration of the wetting liquid into the polymer surface might cause surface swelling and contribute to contact angle hysteresis. This process was reported as a long-term effect depending of the length and size of the liquid molecule.[33−35] Receding contact angles therefore may reflect the resultant of combined effects involving liquid penetration/liquid sorption or liquid retention. Penetration of water into pores at the submicrometer scale was improbable. The hydrostatic pressure ΔP that must be necessary before water penetrates pores with

perimeter "*p*" and area "*A*" can be expressed by the relationship[36]

$$\Delta P = -p\gamma_{LV}(\cos\theta)/A \quad (1)$$

This equation predicts that pressures greater than 10^6 Pa are necessary to cause intrusion of water into pores of 100 nm diameter. Only sorption of molecules of water in the outermost part of the polymer surface can be considered.

Thus, it seems that the hysteresis was mainly caused by molecular interactions between the wetting liquid and the polymer surface and by rearrangement of side groups at the polymer/water interface rather than roughness, variations in chemical composition or surface deformation. It is important to note that the polymer surface reorganization in contact with water is a time-dependent process.[37−39] An immersion gradient may be created between the lower and upper part of the polymer surface during the wetting process. When the polymer surface continues to evolve within the time scale of the dewetting phase, one can observe a curvature of the emersion plateau. Such a phenomenon was not observed with copolymers studied in this work. Sedev et al.[35] reported that relaxation of polymer groups at the surface can be considered as a short-term effect.

In copolymer series p(F8BPH$_m$A-*co*-SMA), reduced wetting hysteresis *H* was found to be higher than that observed for the homologue pSMA homopolymer. Wetting hysteresis tends to decrease with increasing the fluoromonomer content in copolymers. The contact angle hysteresis can be explained by the rearrangement of alkyl and fluoroalkyl side groups at the polymer interface in the presence of water. Rangwalla[40] demonstrated by IR−visible sum frequency-generation spectroscopy the rearrangement and conformational changes of octadecyl side groups of vinyl copolymers when in contact with water. More hydrophilic groups (methylene or ester), buried within the surface in a dry state, were brought out to the surface in contact with water to reduce the surface free energy, which is the driving force of this rearrangement. As shown by DSC and WAXS measurements, the organization of pendent chains can be promoted by structural parameters of the fluorinated monomer (length of the hydrocarbon spacer, perfluoroalkylated biphenyl group) and of the comonomer (octadecyl chain). The polymer surface stability is governed by either the organization of octadecyl side chains or the packing of fluorinated side chains, according to the copolymer composition. For low fluoromonomer content, the stability of the polymer surface is due to packing of the octadecyl side chains. This packing is perturbed by increasing the fluoromonomer content, leading to an augmentation of the wetting hysteresis. With the onset of the organization of fluorinated pendent groups for higher content of fluorinated units (>30 mol %), the wetting hysteresis decreases. This could explain the nonlinear relationship between the wetting hysteresis and copolymer composition. The enhanced organization of octadecyl side groups in p(F8BPH$_m$A-*co*-SMA) series combined with tight packing of perfluoroalkylated chain with a hexamethylene spacer (F8BPH$_6$) can be correlated with the lower contact angle hysteresis observed with the copolymer series p(F8BPH$_6$A-*co*-SMA). Copolymers of this series present a low wetting hysteresis ($\Delta\theta < 20°$) over a large range of compositions. These results showed the influence of the length of hydrocarbon spacer and comonomer alkyl side chain on the wetting hysteresis. The influence of the biphenyl group was evaluated by comparison of contact angle hysteresis ($\Delta\theta = 33°$, $H = 0.264$) obtained for acrylic homopolymers with perfluoroalkylated side groups $C_8F_{17}(CH_2)_6$.[19]

In copolymer series p(F8BPH$_m$A-*co*-MMA), the presence of fluorinated side groups leads to lower contact angle hysteresis than that observed for pMMA. The surface of pMMA is more easily modified by contact with water and presents the highest *H* value. In copolymer series p(F8BPH$_6$A-*co*-MMA) the polymer surface stability is enhanced by the level of perfluoroalkylated side groups as was mentioned previously with SMA copolymer series.

3.2.3. Surface Tension of Fluorinated Acrylic Copolymers. Surface tensions were evaluated using the Lifshitz−van der Waals acid−base theory proposed by van Oss et al.[41] Based on the geometric mean method developed by Fowkes,[42] this approach, stated as method I, can be expressed by the following relationship:

$$\gamma_{SL} = \gamma_S + \gamma_L - 2(\gamma_S^{LW}\gamma_L^{LW})^{1/2} - 2[(\gamma_S^+\gamma_L^-)^{1/2} + (\gamma_S^-\gamma_L^+)^{1/2}] \quad (2)$$

Combining eq 2 with Young's equation leads to

$$\gamma_L(1+\cos\theta) = 2(\gamma_S^{LW}\gamma_L^{LW})^{1/2} + (\gamma_S^+\gamma_L^-)^{1/2} + (\gamma_S^-\gamma_L^+)^{1/2} \quad (3)$$

where γ_S and γ_L are the polymer and liquid surface tensions, γ_i^{LW} is the nonpolar component due to Lifshitz−van der Waals interactions, and γ_i^+ and γ_i^- are the Lewis acid and Lewis base components.

By contact angle (θ_a) measurement with three well-characterized wetting liquids in terms of γ_L^{LW}, γ_L^-, and γ_L^+, using eq 3, the three components of γ_S can be determined. As discussed by Della Volpe et al.,[43] it is possible to control the relevance of the wetting liquid triplets by the condition number (cn) of the matrix **A** used to solve the set of eqs 3 written in the matrix form $A_{3x3}X_{3x1} = b_{3x1}$ where $A = [(\gamma_{Li}^{LW})^{1/2}(\gamma_{Li}^+)^{1/2}(\gamma_{Li}^-)^{1/2}]_{i=1,2,3}$. A low value of the cn ($kA = ||A||\cdot||A^{-1}||$) expresses a well-conditioned matrix and a relevant triplet of wetting liquids. (The 1-norm $||A||_1$ is expressed by $||A||_1 = \max_{1\le j\le n}\sum_{i=1}^{m}|a_{ij}|$). Water and ethylene glycol (EG) were used as polar pair of wetting liquids and diiodomethane or octane as nonpolar liquids as recommended by Good and van Oss.[44] Octane was not used for the copolymer series p(F8BPH$_m$A-*co*-SMA) because the surfaces were not stable in contact with alkanes. The values of *kA* obtained for triplet (water−EG-C_8H_{18}) $kA_1 = 6.10$ and triplet (water−EG-CH_2I_2) $kA_1 = 6.51$ justify the choice of wetting liquids. The two triplets of wetting liquids present similar values for *kA* located in the range corresponding to the set of triplets leading to the most acceptable values of surface tension.[43]

The results obtained for pSMA and fluorinated copolymers with SMA are summarized in Table 2. It should be pointed out that in many cases negative values were obtained for the square root of the γ_S^- component. This occasional occurrence accepted by van Oss et al.[45] has been reported by Kwok and Neumann[46] for fluorinated surfaces. The polar component γ_S^{AB} ($\gamma_S^{AB} = 2(\gamma_S^+\gamma_S^-)^{1/2}$) remained small ($\gamma_S^{AB} \le 0.5$ mN/m) and did not contribute significantly to the surface tension γ_S. As expected for fluorinated acrylic polymers, the surface tension was mainly determined by the Lifshitz−van der Waals component γ_S^{LW}. The surface tension sharply decreased with the presence of few percent of fluoromonomer in the copolymer, leading to very low values (about 7 mN/m) for higher fluoromonomer contents ranging between 30 and 50 mol %. The main structural parameter influencing the nonpolar component was the copolymer composition. The chemical structure of fluorinated side groups (hydrocarbon spacer) did not influence significantly the surface tension.

Table 2. Wetting Behavior and Surface Tensions of Fluorinated Copolymers p(F8BPHmA-*co*-SMA)

fluorinated monomer (mol % in copolymer)	contact angle (deg)			surface tensions (mN/m)				
	H_2O	EG	CH_2I_2	γ_S^{LW}	$(\gamma_S^+)^{1/2}$	$(\gamma_S^-)^{1/2}$	γ_S^{AB}	γ_S
pSMA	108.9	82.0	61.6	27.6	−0.18	0.19	−0.07	27.6
F8BPA (11)	121.5	99.3	97.2	9.7	0.47	0.09	0.08	9.8
F8BPA (31)	126.5	103.4	102.6	7.8	0.54	−0.20	−0.22	7.5
F8BPA (50)	125.7	104.0	103.3	7.5	0.51	−0.04	−0.04	7.5
$F8BPH_6A$ (5)	113.9	88.0	79.2	17.9	0.28	0.1	0.06	18.0
$F8BPH_6A$ (9)	123.0	97.6	88.1	13.6	0.21	−0.34	−0.14	13.4
$F8BPH_6A$ (31)	125.1	103.0	105.9	6.7	0.68	−0.01	−0.01	6.7
$F8BPH_6A$ (50)	125.4	105.0	105.2	6.9	0.51	0.09	0.09	7.0
$F8BPH_{11}A$ (10)	120.1	99.3	97.5	9.6	0.44	0.28	0.25	9.85
$F8BPH_{11}A$ (31)	125.9	103.7	103.3	7.5	0.53	−0.09	−0.09	7.4
$F8BPH_{11}A$ (46)	128.2	104.4	104.6	7.1	0.60	−0.31	−0.37	6.7

Table 3. Contact Angles and Surface Tensions of Fluorinated Copolymers p(F8BPHmA-*co*-MMA) Using as Wetting Liquids Two Triplets: Water−Ethylene Glycol−Diiodomethane and Water−Ethylene Glycol−Octane

fluorinated monomer (mol % in copolymer)	contact angle (deg)			surface tensions (mN/m)				
	H_2O	EG	CH_2I_2/C_8H_{18}	γ_S^{LW}	$(\gamma_S^+)^{1/2}$	$(\gamma_S^-)^{1/2}$	γ_S^{AB}	γ_S
pMMA	78.9	55.0	48.2	35.3	0.27	2.83	1.53	36.8
F8BPA (10)	118.5	96.6	95.6	10.3	0.50	0.35	0.35	10.7
			53.8	13.7	0.15	0.20	0.01	13.7
F8BPA (34)	123.4	102.0	103.9	7.3	0.62	0.11	0.14	7.5
			63.0	11.4	0.12	- 0.01	- 0.00	11.4
$F8BPH_6A$ (9)	124.4	104.7	104.6	7.1	0.48	0.19	0.18	7.3
			68.9	10.0	0.11	0.11	0.02	10.0
$F8BPH_6A$ (31)	127.3	104.8	106.2	6.6	0.62	−0.16	- 0.19	6.4
			70.5	9.6	0.22	−0.25	- 0.11	9.5
$F8BPH_6A$ (50)	124.6	105.1	104.6	7.1	0.46	0.20	0.18	7.3
			68.9	10.0	0.09	0.11	0.02	10.0
$F8BPH_{11}A$ (12)	124.9	102.7	105.5	6.8	0.68	- 0.01	- 0.02	6.8
			66.5	10.6	0.20	−0.12	- 0.05	10.5
$F8BPH_{11}A$ (31)	126.0	104.8	106.5	6.5	0.60	0.01	0.02	6.5
			70.5	9.6	0.19	−0.08	- 0.03	9.6

When the comonomer SMA is substituted by MMA, the results reported in Table 3 showed that the same trend was observed for the various components of the surface tension: (i) some negative values for γ_S^- whatever the nonpolar wetting liquid; (ii) negligible contribution of the acid−base components ($\gamma_S^{AB} \leq 0.35$ mN/m); (iii) very low values for γ_S^{LW} ($\approx$7 mN/m) when diiodomethane was used as wetting liquid. The decrease of γ_S^{LW} as a function of the fluorinated unit ratio was more pronounced in p(F8BPH$_m$A-*co*-MMA) series. Extremely low values of γ_S, ranging between 6.5 and 7.5 mN/m, were obtained with only 10−30 mol % of fluoromonomer. By comparison with results recently published[6] concerning acrylic copolymers (perfluoroalkyl methacrylate-*co*-MMA) with side groups $CH_2C_nF_{2n+1}$, the introduction of a perfluoroalkylated biphenyl group linked to the polymer chain by a hydrocarbon spacer lowered the surface tensions significantly. Surface tensions obtained for copolymers are comparable to values of γ_S reported for methacrylic homopolymers with higher content of pendent fluorinated groups $(CH_2)_2C_nF_{2n+1}$ ($n = 6, 8, 10$).[47] As the polar contribution was not deciding ($\gamma_S^{AB} \leq 0.35$ mN/m), the surface tension was basically controlled by γ_S^{LW} and subsequently by the wettability of the polymer surface by diiodomethane or octane. Diiodomethane that is claimed to be the preferred nonpolar contact angle liquid[44] for determining γ_S^{LW} leads in copolymer series p(F8BPH$_m$A-*co*-MMA) to lower values, reduced by about 3 mN/m by comparison with octane. The problem which has to be considered is the relevance of diiodomethane as wetting liquid for fluorinated surfaces. CH_2I_2 is a polarizable solvent with a dipolar moment ($\mu = 1.1$ D) weak but not equal to zero that induces modification of spectral properties.[48]

To bring more information about the influence of the nature of the nonpolar wetting liquid, surface tensions were determined using the equation of state proposed by Kwok and Neumann.[49] The equation of state for solid−liquid interfacial tension can be written as

$$\gamma_{SL} = \gamma_{SV} + \gamma_{LV} - 2(\gamma_{SV}\gamma_{LV})^{1/2}[1 - \beta(\gamma_{LV} - \gamma_{SV})^2] \quad (4)$$

Combining eq 4 with Young's equation leads to

$$\gamma_{LV}(1 + \cos\theta) = 2(\gamma_{SV}\gamma_{LV})^{1/2}[1 - \beta(\gamma_{LV} - \gamma_{SV})^2] \quad (5)$$

γ_{SV} is obtained from eq 5 by iterative calculation, assuming a constant value for β, determined for fluorinated polymer surface,[50] $\beta = 0.00011354$ (m^2/mJ)^2. Surface tensions reported in Table 4 obtained either by the Lifshitz−van der Waals/acid−base approach (method I) or by the equation of state (method II) were found to be very similar when octane was used as nonpolar liquid. With diiodomethane as wetting liquid, higher values for γ_{SV} were determined by the equation of state approach. Furthermore, the γ_{SV} values calculated by the equation of state were found to be roughly constant (in the range $\pm$ 0.38 mN/m) whatever the nonpolar wetting liquid used (i.e., octane or diiodomethane). These results support the assumption that the discrepancy observed using the Lifshitz−van der Waals/acid−base approach could mainly be attributed to the methodology used for the determination of γ_S and not to the nature of the nonpolar wetting liquid. The approach developed by van Oss et al. based on the geometric mean relationship, proposed by Fowkes,[41] for the determination of the dispersive interactions, seems to be inappropriate to determine accurately the low surface tensions of fluoropolymers. As can be seen in Table 4, there is a systematic trend for the γ_S^{LW} values to decrease as γ_L of the wetting liquid increases, suggesting a severe flaw in this approach.

Table 4. Surface Tensions ($\gamma_S \pm 0.4$ mN/m)[a] of Copolymers p(F8BPHmA-*co*-MMA) Determined by Different Approaches from Contact Angles Obtained Using Nonpolar Wetting Liquids

fluoromonomer (mol %)	wetting liquids	geometric mean relationship γ_S^{LW} (mN/m)	equation of state γ_{SV} (mN/m)	harmonic mean relationship γ_S^{LW} (mN/m)
F8BPA (10)	C_8H_{18}	13.7	13.85	14.3
	CH_2I_2	10.3	14.3	14.8
F8BPA (34)	C_8H_{18}	11.4	11.7	12.3
	CH_2I_2	7.3	10.9	11.9
F8BPH$_6$A (9)	C_8H_{18}	10.0	10.3	11.1
	CH_2I_2	7.1	10.6	11.7
F8BPH$_6$A (31)	C_8H_{18}	9.6	9.8	10.8
	CH_2I_2	6.6	10.0	11.2
F8BPH$_6$A (50)	C_8H_{18}	10.0	10.3	11.1
	CH_2I_2	7.1	10.6	11.7
F8BPH$_{11}$A (12)	C_8H_{18}	10.6	10.85	11.6
	CH_2I_2	6.8	10.3	11.4
F8BPH$_{11}$A (31)	C_8H_{18}	9.6	9.9	10.8
	CH_2I_2	6.5	9.9	11.1

[a] The error limits for γ_{SV} were calculated from the corresponding contact angle errors ($\pm 1°$).

To confirm this statement, surface tensions were evaluated using the harmonic mean relationship introduced by Wu[51] (eq 6).

$$(1 + \cos\theta)\gamma_L = 4\frac{\gamma_S^d \gamma_L^d}{\gamma_S^d + \gamma_L^d} + 4\frac{\gamma_S^p \gamma_L^p}{\gamma_S^p + \gamma_L^p} \qquad (6)$$

As reported in the literature,[52] this approach lead to higher and probably overestimated values of the polar component γ_S^p. Using the harmonic mean relationship to evaluate the γ_S^{LW} component leads to

$$\gamma_S^{LW} = \frac{\gamma_L(1 + \cos\theta)}{3 - \cos\theta} \qquad (7)$$

The influence of the mode of calculation on γ_S^{LW} according to the nonpolar wetting liquid is best illustrated in copolymers series p(F8BPH$_m$A-*co*-MMA). As shown in Table 4, values of γ_S^{LW} derived from the harmonic mean relationship (stated as method III) present only a slight variation as a function of the wetting liquid, octane or diiodomethane. The difference is within the experimental error limits. The same observation that applies in the case of the equation of state is not valid for the geometric mean relationship. The similarity of the results obtained by using both methods II and III (equation of state and harmonic mean relationship) must be underlined.

With the Fowkes approach a regular decrease in γ_S^d as γ_{LV} of the nonpolar wetting liquid increases was mentioned by Kwok et al.[49] for fluorocarbon surfaces. On the basis of recently published data on contact angles of *n*-alkanes and nonpolar liquids with Teflon AF 1600 surfaces,[50] we have calculated the surface tension of Teflon AF using the three approaches (geometric and harmonic mean relationship and equation of state). Using method I, one can observe (cf. Figure 5) that γ_S^{LW} values vary in a regular fashion by about 27% with an increase of γ_{LV}. Values of γ_{SV} calculated with eq 5 fluctuate within a limited range ± 0.65 mN/m. Results obtained with eq 7 present a slight linear increase of γ_S^{LW} with the augmentation of γ_{LV}. Whatever the method used for the calculation, results were found to be convergent when wetting liquids with low surface tensions were used. As illustrated in Figure 5, in the present work the change of γ_S as a function of γ_{LV} shows the same trend.

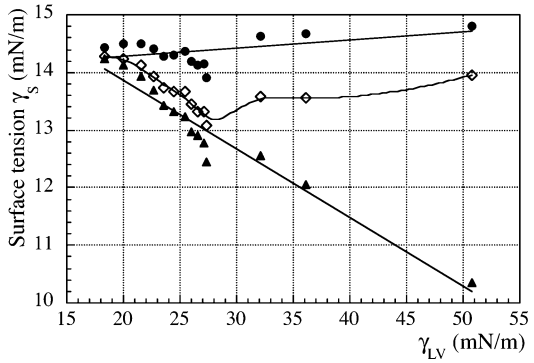

Figure 5. Surface tension of Teflon AF, based on the literature data [*J. Colloid Interface Sci.* **2004**, *279*, 493], determined by different approaches: harmonic mean relationship (●), equation of state (◇), geometric mean relationship (▲).

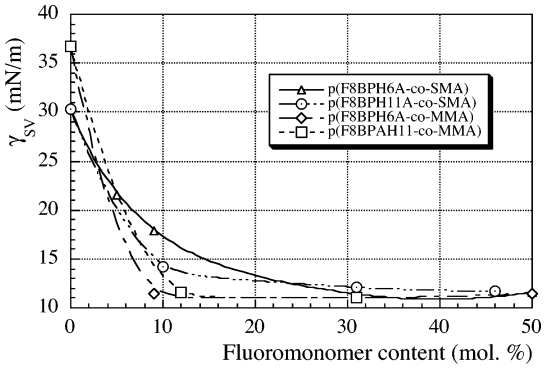

Figure 6. Surface tension of polymers as a function of the mol % of fluorinated monomer unit in the copolymer chain: p(F8BPH$_6$A-*co*-SMA) (△), p(F8BPH$_{11}$A-*co*-SMA) (○), p(F8BPH$_6$A-*co*-MMA) (◇), and p(F8BPH$_{11}$A-*co*-MMA) (□).

Table 5. Surface Tensions ($\gamma_S \pm 0.4$ mN/m) of Copolymers p(F8BPH$_m$A-*co*-SMA) Obtained by Different Approaches Using Diiodomethane as Wetting Liquid

fluoromonomer content (mol %)	geometric mean relationship γ_S^{LW} (mN/m)	equation of state γ_{SV} (mN/m)	harmonic mean relationship γ_S^{LW} (mN/m)
polySMA	27.7	30.45	29.7
F8BPA (11)	9.8	13.7	14.2
F8BPA (31)	8.0	11.4	12.3
F8BPA (50)	7.6	11.15	12.1
F8BPH$_6$A (5)	18.0	21.9	21.45
F8BPH$_6$A (9)	13.7	17.7	17.7
F8BPH$_6$A (31)	6.7	10.1	11.3
F8BPH$_6$A (50)	7.0	10.4	11.5
F8BPH$_{11}$A (10)	9.85	13.5	14.1
F8BPH$_{11}$A (31)	7.6	11.15	12.1
F8BPH$_{11}$A (46)	7.5	10.6	11.7

Different methods were used to determine the polymer surface tensions in p(F8BPH$_m$A-*co*-SMA) series. As seen in Table 5, the results obtained either with method II or III are in relative good agreement within experimental errors. As concluded by Correia et al.,[53] the range of application of the equation of state must be restricted to nonpolar liquids.

The sharp decrease in surface tension of the copolymers with increasing the ratio of fluorinated unit points up the influence of both the comonomer type (MMA or SMA) and the chemical structure of fluorinated side group (cf. Figure 6) on the surface properties. This was mainly observed with copolymers with low fluoromonomer content. On the basis of a structural analysis, one can suggest that fluorinated side groups are partly masked by the longer side chains of SMA units.

Fluorinated side groups with hydrocarbon spacers $(CH_2)_6$ or $(CH_2)_{11}$ were found to contribute more efficiently in lowering the surface tension. The lowest surface tension values ($\gamma_{SV} \approx 11$ mN/m) were reached for lower content of fluorinated unit in the copolymers series p(F8BPH$_6$A-*co*-MMA) and p(F8BPH$_{11}$A-*co*-MMA). In the p(F8BPH$_m$A-*co*-MMA) series, low surface tensions seemed to be obtained at the expense of the polymer surface stability. As shown previously, polymer surfaces in p(F8BPH$_m$A-*co*-SMA) series were found more resistant to disorganization in the presence of polar wetting liquid. These results underline the difficulties, in polymer surface tailoring, in finding the structural parameters able to reconcile low surface tension and wetting stability.

4. Conclusions

The surface properties of new acrylic copolymers, containing fluorinated side groups with a biphenyl core and hydrocarbon spacers of different length, were investigated by dynamic contact angle measurements. The advancing contact angles with water were independent of the side chain chemical structure and were almost constant ($\theta_a \approx 125°$) as long as the fluoromonomer content exceeded 10 mol %. Surface tensions of the copolymers dropped rapidly as the fluoromonomer content increased and reached markedly lower values than those of corresponding alkyl substituted homopolymers. Compared with fluorinated aliphatic analogues, the presence of perfluoroalkylated biphenyl side groups drastically reduced wetting hysteresis of the polymer films. This is a consequence of the self-organization of side groups evidenced by X-ray scattering. The wetting hysteresis was attributed to the reorganization of side chains occurring in the outermost part of the polymer surface due to the contact with water. The wetting hysteresis was minimized by the presence of either fluorinated or octadecyl side chains. The cohesion between fluorinated side chains was improved by the presence of the biphenyl core. Surface tensions of nonpolar fluoropolymers were better estimated by the equation of state or the harmonic mean relationship. These approaches provided reasonable and consistent surface tension values far less dependent on the wetting liquids than the results obtained from the acid−base theory.

Acknowledgment. The authors thank Mrs. Valerie Flaud for the surface analysis by AFM and Dr. Vincent Cavalier for fruitful discussions on matrix calculations.

References and Notes

(1) Boutevin, B.; Pietrasanta, Y. In *Les acrylates et polyacrylates fluorés. Dérivés et applications;* Erec Ed: Paris, 1988; Chapter 7.
(2) Scheirs, J. In *Modern Fluoropolymers*; John Wiley: New York, 1997; pp 1−69.
(3) Park, I. J.; Lee, S. B.; Choï, C. K.; Kim, K.-J. *J. Colloid Interface Sci.* **1996**, *181*, 284−288.
(4) Kassis, C. M.; Steehler, J. K.; Betts, D. E.; Guan, Z.; Romack, T. J.; DeSimone, J. M.; Linton, R. W. *Macromolecules* **1996**, *29*, 3247−3254.
(5) Thomas, R. R.; Anton, D. R.; Graham, W. F.; Darmon, M. J.; Sauer, B. B.; Stika, K. M.; Swartzfager, D. G. *Macromolecules* **1997**, *30*, 2883−2890.
(6) van de Grampel, R. D.; Ming, W.; van Gennip, W. J. H.; Laven, J.; Niermantsverdriet, J. W.; Brongersma, H. H.; de With, G.; van der Linde, R. *Langmuir* **2004**, *20*, 6344−6351.
(7) Katano, Y.; Tomono, H.; Nakajima, T. *Macromolecules* **1994**, *27*, 2342−2344.
(8) Marchionni, G.; Ajroldi, G.; Righetti, M. C.; Pezzin, G. *Macromolecules* **1993**, *26*, 1751−1757.
(9) Finkelmann, H.; Ringsdorf, H.; Wendorff, J. H. *Makromol. Chem.* **1978**, *179*, 273−276.
(10) Finkelmann, H.; Rehage, G. *Adv. Polym. Sci.* **1984**, *60/61*, 99−172.
(11) Kitazume, T.; Ohnogi, T. *J. Fluorine Chem.* **1990**, *47*, 459−466.
(12) Kitazume, T.; Ohnogi, T.; Ito, K. *J. Am. Chem. Soc.* **1990**, *112*, 6608−6615.
(13) Ruhmann, R.; Thiele, T.; Wolff, D.; Prescher, D.; Springer, *J. Liq. Cryst.* **1996**, *21*, 307−312.
(14) Wolff, D.; Ruhmann, R.; Thiele, T.; Prescher, D.; Springer, *J. Liq. Cryst.* **1996**, *20*, 553−557.
(15) Thiele, T.; Prescher, D.; Ruhmann, R.; Wolff, D. *J. Fluorine Chem.* **1997**, *85*, 155−161.
(16) Andruzzi, L.; D'Apollo, F.; Galli, G.; Gallot, B. *Macromolecules* **2001**, *34* 7707−7714.
(17) Magagnini, P. L. *Makromol. Chem., Suppl.* **1981**, *4*, 223−240.
(18) Shibaev, V. P.; Freidzon, Ya. S.; Kostromin, S. G. In *Liquid Crystalline and Mesomorphic Polymers*; Shibaev, V. P., Lam, L., Eds.; Springer-Verlag: NewYork, 1984; Chapter 3.
(19) Melas, M. In *Alcools perfluoroalkylés et Polyacrylates dérivés. Synthèse, étude structurale et propriétés de Surface.* Thesis of doctorat, Université Montpellier II, Montpellier, France, 1995.
(20) Morita, M.; Ogisu, H.; Kubo, M. *J. Appl. Polym. Sci.* **1999**, *73*, 1741−1749.
(21) Hartmann, P. C.; Collet, A.; Viguier, M.; Blanc, C. *J. Fluorine Chem.* **2004**, *125*, 1909−1918.
(22) van Oss, C. J. *J. Adhes. Sci. Technol.* **2002**, *16*, 669−677.
(23) Neumann, H. J.; Jarek, M.; Hellmann, G. P. *Macromolecules* **1993**, *26*, 2489−2495.
(24) Neumann, A. W.; Good, R. J. *J. Colloid Interface Sci.* **1972**, *38*, 341−358.
(25) Busscher, H. J.; van Pelt, A. W. J.; de Boer, P.; de Jong, H. P.; Arends, *J. Colloids Surf.* **1984**, *9*, 319−331.
(26) de Gennes, P. G. *Rev. Mod. Phys.* **1985**, *57*, 827−863.
(27) Lam, C. N. C.; Wu, R.; Li, D.; Hair, M. L.; Neumann, A. W. *Adv. Colloid Interface Sci.* **2002**, *96*, 169−191.
(28) Sedev, R. V.; Budziak, C. J.; Petrov, J. G.; Neumann, A. W. *J. Colloid Interface Sci.* **1993**, *159*, 392−399.
(29) Hayes, R. A.; Ralston, J. *J. Colloid Interface Sci.* **1993**, *159*, 429−438.
(30) Extrand, C. W.; Kumagai, Y. *J. Colloid Interface Sci.* **1995**, *170*, 515−521.
(31) Extrand, C. W.; Kumagai, Y. *J. Colloid Interface Sci.* **1997**, *191*, 378−383.
(32) Erbil, H. Y.; McHale, G.; Rowan, S. M.; Newton, M. I. *Langmuir* **1999**, *15*, 7378−7385.
(33) Lam, C. N. C.; Ko, R. H. Y.; Yu, L. M. Y.; Ng, A.; Li, D.; Hair, M. L.; Neumann, A. W. *J. Colloid Interface Sci.* **2001**, *243*, 208−218.
(34) Lam, C. N. C.; Kim, N.; Hui, D.; Kwok, D. Y.; Hair, M. L.; Neumann, A. W. *Colloids Surf., A* **2001**, *189*, 265−278.
(35) Sedev, R. V.; Petrov, J. G.; Neumann, A. W. *J. Colloid Interface Sci.* **1996**, *180*, 36−42.
(36) Youngblood, J. P.; McCarthy, T. J. *Macromolecules* **1999**, *32*, 6800−6806.
(37) Yasuda, T.; Miyama, M. *Langmuir* **1994**, *10*, 583−585.
(38) Tretinnikov, O. N.; Ikada, Y. *Langmuir* **1994**, *10*, 1606−1614.
(39) Varennes, S.; Schreiber, H. P. *J. Adhes.* **2001**, *76*, 293−306.
(40) Rangwalla, H.; Schwab, A. D.; Yurdumakan, B.; Yablon, D. G.; Yeganeh, M. S.; Dhinojwala, A. *Langmuir* **2004**, *20*, 8625−8633.
(41) van Oss, C. J.; Chaudhury, M. K.; Good, R. J. *Chem. Rev.* **1988**, *88*, 927−941.
(42) Fowkes, F. M. *J. Phys. Chem.* **1963**, *67*, 2538−2541.
(43) Della Volpe, C.; Maniglio, D.; Brugnara, M.; Siboni, S.; Morra, M. *J. Colloid Interface Sci.* **2004**, *271*, 434−453.
(44) Good, R. J.; van Oss, C. J. In *Modern Approaches to Wettability*; Schrader, M. E., Loeb, G. I., Eds.; Plenum Press: New York, 1992; pp 1−27.
(45) Wu, W.; Giese, R. F., Jr.; van Oss, C. J. *Langmuir* **1995**, *11*, 379−382.
(46) Kwok, D. Y.; Neumann, A. W. *Adv. Colloid Interface Sci.* **1999**, *81*, 167−249.
(47) Tsibouklis, J.; Graham, P.; Eaton, P. J.; Smith, J. R.; Nevell, T. G.; Smart, J. D.; Ewen, R. J. *Macromolecules* **2000**, *33*, 8460−8465.
(48) Menger, F. M.; Sanchez, A. M. *Chem. Commmun.* **1997**, 199−200.
(49) Kwok, D. Y.; Li, D.; Neumann, A. W. *Langmuir* **1994**, *10*, 1323−1328.
(50) Tavana, H.; Lam, C. N. C.; Grundke, K.; Friedel, P.; Kwok, D. Y.; Hair, M. L.; Neumann, A. W. *J. Colloid Interface Sci.* **2004**, *279*, 493−502.
(51) Wu, S. *J. Macromol. Sci., Rev. Macromol. Chem.* **1974**, *10*, 1−73.
(52) *J. Colloid Interface Sci.* **1989**, *127*, 189−204.
(53) Correia, N. T.; Moura Ramos, J. J.; Saramago, B. J. V.; Calado, C. G. *J. Colloid Interface Sci.* **1997**, *189*, 361−369.

MA060894T